Phenomenology of γ-irradiation-induced changes in optical properties of chalcogenide semiconductor glasses: a case study of binary arsenic sulfides

M. Shpotyuk[1], A. Kovalskiy[2], R. Golovchak[2] and O. Shpotyuk[3,4*]

[1] Lviv Polytechnic National University, 12 Bandera str., Lviv, 79013, Ukraine

[2] Department of Physics and Astronomy, Austin Peay State University, Clarksville, TN 37044, USA

[3] Vlokh Institute of Physical Optics, 23 Dragomanov str., Lviv, 79005, Ukraine

[4]Jan Dlugosz University of Czestochowa, 13/15 al. Armii Krajowej, Czestochowa, 42-200, Poland

Abstract.

Two methodological approaches to describe changes in the optical transmission spectra of chalcogenide semiconductor glasses induced by high-energy γ-irradiation are considered at the example of glassy arsenic sulfides. The studied radiation-optical effects are ascribed to destruction-polymerization transformations, both intrinsic and related to surface oxidation. Direct-chronology *ex-situ* and backward-chronology *in-situ* measuring protocols can be utilized to parameterize them in glasses, while the former includes unresolved input from natural and radiation-assisted physical ageing in addition to mismatch between control and reference glasses. The reliable signature of intrinsic radiation-optical phenomenology unbiased by competitive input from oxidation and physical ageing is provided with *in-situ* measurements for the same irradiated glass.

The developed approaches are probed for glassy $As_{40}S_{60}$ and $As_{30}S_{70}$, which demonstrate principally different responses on radiation-structural transformations and accompanied physical ageing. Critical assessment is given on misleading speculations ignoring intrinsic changes in view of competitive contribution from radiation-induced surface oxidation and thermally-assisted ageing. Stoichiometric As_2S_3, showing dramatic changes in optical transmission spectra, is nominated as canonical model object among chalcogenide glasses revealing highest sensitivity to γ-irradiation. These methodological solutions are in excellent agreement with structure-modification criteria developed to parameterize compositional trends in radiation-optical response of chalcogenide glass.

Keywords: chalcogenide glass, radiation-optical effects, γ-irradiation, oxidation, physical ageing

*Corresponding author. Tel.: +38 032 2631065

E-mail address: olehshpotyuk@yahoo.com (Oleh Shpotyuk)

1. Background

Methodological problems related to radiation-induced metastability in glassy chalcogenides

Influence of high-energy ionizing irradiations on structure and properties of *chalcogenide semiconductor glasses* (ChSGs), or so-called *radiation-induced effects* (RIEs) has been in a sphere of tight interests of materials scientists since the earliest 1960s, the time of the pioneering research initiated by I.A. Domoryad on γ-irradiation response in mechanical and optical properties of glassy g-Se, g-$As_{40}S_{60}$ and g-$As_{40}Se_{60}$ [1-3]. In the following decades of the 1970-1980s, the microstructure mechanism of radiation metastability in ChGS-forming systems became a subject of scrupulous study in view of their potential applications in industrial sensorics and irradiation-guided structure-modification technologies (see, e.g. ref. [4] and literature therein).

The problem of radiation-induced metastability in the ChSG-forming systems concerns, in fact, the nature of structural defects in high-entropy disordered state caused by disturbance of existing chemical bonds, and followed by relaxation towards structural state with new bond distribution. Within a common opinion, such structural modification (SM) can be ascribed to *destruction-polymerization transformations* (DPTs) [4-14], meaning that metastability is related to novel bond distribution in a glassy network obeying full saturation of covalent bonding in respect to the Mott's (8–*N*) rule [7]. It seems understandable, that chemical bonds destroyed in ChGS by irradiation can be restored *intrinsically* via direct interaction of bond-constituting atoms with nearest neighbors (intrinsic bond switching), or *extrinsically* owing to interaction with impurities absorbed from an environment. In the former case, the pairs of diamagnetic over- and under-coordinated atoms possessing an excess of positive and negative electrical charge, respectively, named *coordination*

topological defects (CTDs), appear in the irradiated ChSGs [4,8-14]. Alternatively, this process proceeds as non-defective DPT, provided two bonds are switched simultaneously [15]. The impurity dopants appear under extrinsic saturation of destructed chemical bonds, this occurring preferentially at the surface of ChSGs [4,16]. The most essential impurity effect can be produced by interaction with absorbed oxygen atoms (radiation-induced oxidation), replacing chalcogen in different bonding configurations in a glassy network. In case of As-based ChSGs, formation of arsenolite As_4O_6 crystallites is favorable and almost independent on chalcogen type [4,17,18]. Typically, *intrinsic* and *extrinsic* (impurity-related) DPTs occur together, forming complicated picture of competitive inputs in overall RIE. Since the ChSGs are always in thermodynamically metastable state characterized by an excess of configurational entropy, enthalpy and/or free volume, they tend with time towards extrapolated state of supercooled liquid, this structural relaxation being called *physical ageing* [19-26]. This process is known to be distinguish as *natural physical ageing*, when occurring under ambient conditions (at room temperature), or *induced physical ageing*, when occurring under external influences (such as photoexposure, irradiation, elevated temperatures, etc.) [25,26]. Possibility of high-energy irradiation to affect the physical ageing especially in chalcogen-rich glassy networks [26,27] introduces an additional ambiguity in the observed RIE. Also, the correct chronology protocol of the experiment has to be used to capture *static* (residual) and *dynamic* (decaying with time after irradiation finishing) RIE components [4].

These complications make an important problem on reliable methodology allowing unbiased separation of contributions in an overall RIE, especially for implementation of irradiation-modified ChSGs. Scrupulous methodological analysis is also crucial in view of recent publications [28-30] trying to give a simplified interpretation of RIEs without distinguished inputs from all alternative sources. So, at the present, an actual challenge is to identify unambiguously the intrinsic RIEs in the ChSGs, separating competitive contributions from accompanied oxidation and physical ageing.

In these methodological notes, we'll present a case of adequate solution of this problem based on more than half-century experience in the RIEs study for archetypal binary g-As-S system, and propose the SM criteria parameterizing radiation-optical response in different ChSG systems.

2. Experimental

2.1. Samples preparation, radiation treatment and optical characterization

Two representative samples of g-As_xS_{100-x} system were selected, these being stoichiometric g-$As_{40}S_{60}$ possessing high sensitivity to RIEs [4,9-11] but no radiation-induced physical ageing and S-rich g-$As_{30}S_{70}$ with pronounced ability to radiation-induced physical ageing [26,31-33].

The ChSG samples were prepared by melt-quenching route using respective quantities of high-purity elemental ingredients, i.e. As (*Alfa-Aesar*, 99.99999%) and S (*ASARCO*, 99.999%), as described in more details elsewhere [31-33]. For optical studies, the glassy specimens were cut as plane-parallel discs (having ~1.5 mm in a thickness and ~10.0 mm in a diameter), and carefully polished to high optical quality with alumina abrasives. Before irradiation, the samples were annealed at 20 K below glass transition temperature T_g to eliminate stress in a bulk frozen at rapid quenching. So the g-As_xS_{100-x} samples prepared for irradiation can be characterized as *thermally-aged* ones, i.e. preliminary affected to below-T_g thermally-assisted physical ageing [26].

The γ-irradiation was carried out at ambient conditions of stationary ^{60}Co radiation field (with an average energy of E=1.25 MeV). The duration of γ-irradiation treatment (up to 6 months) allows accumulate a total dose up to 10 MGy (in the current case, this dose was about 3.0 MGy). Temperature effect during such prolonged γ-irradiation was not essential, since the maximum temperature in the spectrometer chamber did not exceed 310 K.

Optical transmission spectra of the ChSGs samples were recorded in a region of their fundamental absorption edge (450-1000 nm) using fiber-optics "AvaSpec-2048" (Avantes, the Netherlands), and double-beam "Specord M-40" (Carl Zeiss, Germany) and "Lambda-35" (Perkin-Elmer) spectrometers. The uncertainty in optical transmission measurements did not exceed ±0.2%. Optical measurements were performed few days after γ-irradiation and, at least, one month later. In such a way, the dynamic RIEs [4,34] were excluded, and only static RIEs were parameterized.

2.2. On the methodological diversity in RIEs detection

Two principally different measuring protocols depicted on Fig. 1 can be used to detect the RIEs, these being realized within (i) continuous *in-situ* measurements in *direct* or *backward* chronology for the same control sample affected by irradiation or (ii) discontinues cycles of *ex-situ* measurements for one control ChGS sample before and after irradiation, or two different samples, one being *control* (irradiated) and other being *reference* (unirradiated).

The discontinues *ex-situ* optical measurements can be arranged in *direct* chronology for the same ChSG sample taken in growing step-by-step sequence of the following structural states:

(1) initial state (i.e. unirradiated sample taken just before irradiation);

(2) γ-irradiated state (the former sample taken after irradiation finishing);

(3) near-T_g thermally-annealed (i.e. deeply aged [26] or very long aged [22]) state;

(4) rejuvenated (i.e. affected to over-T_g heating-cooling cycle [26]) or as-prepared state.

Each of these stages is important to completely represent *optical signature* of RIE in the ChSG, while inputs from intrinsic and impurity-related DPTs cannot be resolved adequately in this route, unless the sample is completely cleaned from products of radiation-induced surface oxidation [27]. To minimize errors originated from discontinuity of *ex-situ* optical measurements (within a few months duration of γ-irradiation), the special marks on the sample's surface are necessary to restore its position in respect to probe light beam as precise as possible (before and after γ-irradiation).

However, this direct-chronology *ex-situ* procedure is ineffective for too prolonged measuring cycles, when instrumentation errors of optical detecting systems may be subjected to essential changes in an uncontrolled manner. In addition, the contribution of natural physical ageing in the irradiated ChSG cannot be adequately resolved within this approach. Thus, the measured optical data concern, in fact, the cumulative input from (i) RIE itself, (ii) natural physical ageing, and (iii) non-reproducibility of optical detecting system.

To avoid uncontrolled time drift in optical detectors, *ex-situ* measurements can be arranged for two identical ChSG samples taken as *control* (i.e. irradiated) and *reference* (i.e. unirradiated) ones. In this case, the similarity between two samples should be precisely controlled at each stage, because any difference becomes source of error in addition to unresolved contribution from radiation-assisted physical ageing (see Fig. 1).

Within *in-situ* measurements arranged in *backward chronology*, the optical transmission spectra are recorded for the same γ-irradiated sample used to reproduce the following states:

(1) irradiated state (i.e. the ChSG sample taken just after irradiation);

(2) annealed state (i.e. the same irradiated sample annealed directly in spectrometer chamber);

(3) rejuvenated state (i.e. the same ChSG sample subjected to rejuvenation procedure by over-T_g heating-cooling cycle [26]).

The best reliability in radiation-optical phenomenology is provided within this backward-chronology *in-situ* measuring owing to complete elimination of errors, associated with accurate sample positioning in a spectrometer chamber and too prolonged time gaps between optical measurements for tested ChSG sample taken in different states. The contribution of impurity-related and intrinsic DPTs can be simply separated within this measuring protocol for the same γ-irradiated sample taken with cleaned or uncleaned surfaces. Since oxidation is most important just under irradiation, we deal practically with the same oxidized ChSG sample affected to post-irradiation thermal treatments (such as near-T_g thermal annealing and/or rejuvenation), when all changes occur due to intrinsic DPTs (so we can ignore the impurity-related effects such as radiation-induced oxidation in the detected changes).

Unfortunately, the *in-situ* optical measurements cannot be simply realized in *direct chronology* because of obvious difficulties in the recording optical transmission spectra for ChGS sample affected to γ-irradiation and different thermal-treatment procedures just in the irradiation chamber (i.e. in the conditions of stationary ^{60}Co radiation field).

3. Results and discussion

3.1. RIEs by direct-chronology *ex-situ* measurements

Optical transmission spectra of the same g-$As_{40}S_{60}$ sample measured *ex-situ* in direct chronology, i.e. before and after γ-irradiation with 3.0 MGy dose and subsequent post-irradiation thermal treatments are shown in Fig. 2.

The detected long-wave shift in optical transmission of γ-irradiated glass corresponds to so-called radiation-induced *darkening* [4] originated from both *intrinsic* and *impurity-related* DPTs, which cannot be resolved unambiguously under *ex-situ* measuring protocol. Further thermal annealing at the temperatures approaching glass transition temperature T_g tends the optical transmission of the irradiated glass towards the initial state 1.2 (Fig. 2), revealing threshold-like behavior [4,35,36]. The restoration is only partial because of the competitive contribution from radiation-induced oxidation. Thus, the thermally-aged states for initial (solid-black curve, Fig. 2) and irradiated non-cleaned sample (thin-black curve, Fig. 2) essentially differ in spectral positions and optical transmittances. These states coincide for irradiated and initial samples only after removing the oxidized layer. Intrinsic and impurity-related DPTs cannot be separated reliably in direct-chronology *ex-situ* experiments because of difference in thermal effect for pure and oxidized ChSGs. Hence, the only solution is to remove the oxidized layer from the surface of γ-irradiated ChSG and repeat measurements for this cleaned sample within the same thermal-treatment cycles.

Fortunately, such solution is simply possible for g-As-S, since arsenolite As_4O_6 layer appeared at the sample's surface due to oxidation under γ-irradiation can be easily removed by wet cleaning [4,18,27,37,38]. Such arsenolite crystallites act as effective scattering centers reducing optical transmission in near-bandgap region (due to Rayleigh scattering), as well as in mid-IR transmission region (preferentially due to Mie scattering losses) [39,40]. This feature is well illustrated by Fig. 2 showing two different transmission curves for the same uncleaned (state 2.2) and cleaned γ-irradiated sample (state 2.1). It is seen that not only saturation level (i.e. optical transmittance), but also slope of transmission edge are essentially modified in uncleaned γ-irradiated g-$As_{40}S_{60}$ sample due to oxidation. The shadowed space between these curves corresponding to thermally-aged states 1.2 and 3.2 (see Fig. 2) reproduces the region of unpredictable deviations in optical measurements, which cannot be repeated reliably within this measuring protocol.

Noteworthy, such solution is unacceptable for Ge-based ChSGs like g-Ge-As-S [4,41,42], where the residual Ge-oxidation effect cannot be eliminated by wet cleaning due to insolubility of GeO_x species [43]. For Ge-based ChSGs studied within direct measuring chronology and even cleaned after irradiation, we have been never able to distinguish between intrinsic and impurity-related RIEs like it was in g-As-S. That is why recent allegations nominating g-$Ge_{15.8}As_{21}S_{63.2}$ as "the best model object" for RIEs in ChSGs [28-30] seems to be completely doubtful.

Thus, the direct-chronology measurements have many disadvantages due to time separation and uncertainties between subsequent cycles of optical transmission spectra recording for initial (thermally-annealed or rejuvenated) and γ-irradiated (cleaned or uncleaned) samples. Simultaneous measurements for two ChSG samples (unirradiated and γ-irradiated) allows only partial solution, since it is impossible to prepare such samples, which will be exactly the same in all aspects. Therefore, the optimal methodology for intrinsic RIEs detection is to arrange the measuring cycles for the same ChSG sample, ensuring as short as possible time gaps between its different states.

With respect to optical transmission spectra of g-$As_{40}S_{60}$ measured *ex-situ* in direct chronology for different states (compare optical spectra in states 1.2, 2.2 and 3.2 on Fig. 2), it worth to underline that incomplete elimination of the oxidized layer results only in partial restoration. It means that γ-irradiated ChSGs with some remnants of oxidation products is in a more darkened state as compared to initial one. This finding is of high importance for ChSG tested in multiple irradiation-annealing cycles. Indeed, in this case, preliminary γ-irradiated samples affected to either thermal annealing or slow heating-cooling treatment (the rejuvenation procedure) differ from initial ones not affected by γ-irradiation. Just this incomplete removing of oxidized surface layer along with prolonged time intervals between separate measurements, sometimes exceeding a decade (i.e. more than ten years after irradiation finishing, thus allowing very-long physical ageing), causes a situation, when totally

incomparable optical transmission spectra are detected for the same g-$As_{40}S_{60}$ sample in different experiments [28,29].

In an obvious contrast, the unprecedented example of correct direct-chronology *ex-situ* methodological approach gives experimental research on reversible photoinduced changes in intermolecular distance in amorphous As_2S_3 films performed by K. Tanaka more than four decades ago [44]. The author used a set of identical films (deposited within the same technology), illuminated by the same photon flux (at 77 and 290 K) in 10^{-5} Torr vacuum to avoid photooxidation, and performed all XRD measurements in the same point-accumulation regime to improve reproducibility of the results separated by relatively long time intervals between measurements.

3.2. RIEs by backward-chronology *in-situ* measurements

Optical measurements in *backward chronology* for the same γ-irradiated ChSG sample provides breakthrough solution in the RIEs phenomenology. Within this approach, the RIE is described due to difference in optical transmission between γ-irradiated and subsequently annealed ChSG sample. The measuring protocol is based on predisposition that near-T_g heating erases intrinsic γ-induced effect, restoring initial structure of unirradiated ChSG [4,31,35]. To ensure high accuracy, all post-irradiation measurements are performed *in-situ*, i.e. the control γ-irradiated ChSG sample is kept in the same position in respect to the probe-light beam during all post-irradiation treatments. Thus, *backward-chronology in-situ* measurements allow to avoid inaccuracies associated with sample positioning in spectrometer chamber. To distinguish intrinsic and impurity-related RIEs, the cleaned ChSGs free of radiation-induced oxidation products are to be used.

As an example, Fig. 3a shows optical transmission spectra of preliminary cleaned g-$As_{40}S_{60}$ recorded *in-situ* in a backward chronology, i.e. in a sequence from γ-irradiated state (curve 1), then thermally aged at 20 K below T_g state (curve 2) to further rejuvenated state (curve 3). Strong *bleaching* effect is evident for this γ-irradiated sample as a result of thermal annealing (transition from optical transmission curve 1 to 2, Fig. 3a) in full respect to [4,35], followed by *darkening* after rejuvenation (transition from optical transmission curve 2 to 3, Fig. 3a). The optical transmission spectra of g-$As_{40}S_{60}$ differ essentially in these states, providing information on magnitudes of intrinsic RIEs and thermally-assisted physical ageing.

Because competitive effect of γ-induced oxidation is simply excluded owing to wet cleaning, the observed changes (Fig. 3a) can be attributed to "pure" DPTs related to redistribution of bonds. Thus, the g-$As_{40}S_{60}$ indeed serves as best canonical model object to study RIEs in ChSGs.

As a counterexample, let's consider the similar changes in optical transmission spectra for non-stoichiometric g-$As_{30}S_{70}$ (Fig. 3b) possessing high propensity to below-T_g structural relaxation [31]. This sample demonstrates negligible γ-induced effect (curve 1, Fig. 3b) in respect to thermally-aged state (curve 2, Fig. 3b), despite considerable physical ageing for both states as compared with rejuvenated one (curve 3, Fig. 3b). These peculiarities are in excellent agreement with known compositional behavior of physical ageing in floppy networks of chalcogen-rich ChGSs [31,26,45], just overriding the γ-irradiation-induced DPTs responsible for intrinsic RIEs in this domain [4,31].

The evident advantages of such arranged measurements can be also well illustrated with famous Keiji Tanaka's *in-situ* experiment on photoinduced changes in g-As_2S_3 installed directly on goniometer, showing the asymmetry of the first sharp diffraction peak [46].

3.3. On the compositional dependence of RIEs in g-As-S

Within comprehensive methodological consideration of RIEs in ChSGs caused by prolonged γ-irradiation at ambient conditions, it is important to note that *in-situ* measuring protocol should be arranged in *backward chronology* in respect to post-irradiation thermal annealing and rejuvenation procedures (as sketched in Fig. 1) to identify unambiguously contributions from intrinsic radiation-induced DPTs and all accompanied inputs. The physical meaning of this simple statement is convincingly evident from Fig. 4 showing compositional behavior of RIEs in g-As_xS_{100-x} detected *in-situ* in *backward chronology* (the studied samples were irradiated with 0.7 kGy/h dose rate at ambient conditions and 3 MGy accumulated dose, as it was described in details elsewhere [31]). After

irradiation, these ChSGs were carefully cleaned from oxidation products, and only then subjected to thermal annealing near glass transition temperature T_g and subsequent heating-cooling rejuvenation procedure. The resulting curves shown in Fig. 4 correspond to the difference between sample's optical transmission (measured *in-situ* in backward chronology) in annealed (thermally-aged) or rejuvenated state and γ-irradiated state. It is clearly seen that radiation-induced darkening effect is proper to the thermally-aged close-to-stoichiometry g-As_xS_{100-x} samples (x=36, 40, 42). If compared to the rejuvenated (i.e. non-aged) ChSGs, only g-$As_{40}S_{60}$ and g-$As_{42}S_{58}$ reveal radiation darkening, while others (x=36, 33, 30) are dominated with blue-shifted optical transmission.

Noteworthy, strong dependence of irradiation response on pre-history of g-$As_{36}S_{64}$ sample can be concluded from Fig. 4, e.g. darkening is observed for thermally-aged sample and bleaching for the rejuvenated (as-prepared) one. Within *ex-situ* measurements arranged as stated in [14,17], i.e. irrespectively to thermal pre-history effects, this sample can demonstrate either one of these responses in its radiation sensitivity. In fact, such "strange" behavior is caused by overlapped contributions from intrinsic DPTs (causing *red shift* in fundamental optical absorption edge) and radiation-assisted physical ageing (causing *blue shift* in fundamental optical absorption edge), which can be reliably resolved within *in-situ backward-chronology measurements*, thus giving a quite reasonable explanation of this anomaly in terms of developed physical models [4-12].

3.4. On the parameterized SM efficiency in ChSGs

The methods of SM of ChSGs using external factors such as high-energy γ-irradiation offer new opportunities to achieve their better functionality. That is why development of SM criteria for ChSGs is an important practical task in view of growing interest to these materials.

Previously, this problem was addressed by A.I. Popov [47-50], who was the first giving explanation for *transient* RIEs occurring just under irradiation. However, this approach is unable to account for the effects of post-irradiation *structural relaxation* resulting in *dynamic* and *static* components of RIEs. We assume that static component of metastable RIEs is related to DPTs, which are connected with permanent switching of covalent chemical bonds in ChSG matrix, accompanied by CTDs formation [4-14,51]. The initiating bond-destructive action is defined by energy transferred into the irradiated sample due to external influence (photoexposure, high-energy ɣ-irradiation, irradiation with accelerated particles, etc.). It is possible to consider all variants of such DPTs in dependence on ChSG chemistry [4,52], and select the most probable ones responsible for the observed residual RIEs.

So, it seems reasonable to introduce the SM criterion for residual RIEs in ChSG (i.e. the κ parameter reflecting directly the magnitude of radiation-induced optical changes) as product of similar parameters describing transient *in-situ* RIEs (κ_1) calculated after Popov [47-50]) and post-irradiation structural relaxation (κ_2):

$$\kappa = \kappa_1 \cdot (1 - \kappa_2) \qquad (1)$$

By allowing variety of both κ_1 and κ_2 parameters from 0 to 1, the SM criterion can be defined within the same variation domain. In respect to eq. (1), the $\kappa = 0$ or absence of residual changes (static component) corresponds to negligible contribution from transient changes, when κ_1 approaches 0, or, alternatively, very strong relaxation input, when κ_2 approaches 1. On the contrary, the $\kappa = 1$ corresponds to strongest residual SM occurring under essential transient changes ($\kappa_1 = 1$) in ChSGs possessing negligible relaxation ($\kappa_2 = 0$). Among all known ChSGs, the maximum κ_1 value is attributed to g-Se, which does not demonstrate any stable residual γ-induced changes at room temperature [47]. In the same manner, the SM criterion increases in As_2S_3 – As_2Se_3 – As_2Te_3 row, despite an obvious decaying tendency for metastable RIEs in this sequence [4,52-54].

The γ-induced DPTs are revealed in the ChSG-forming networks owing to misbalance in covalent bonding, local atomic coordination and intrinsic electrical field [4-14]. Therefore, the overall contribution of structural relaxation to the metastable RIEs arises from corresponding inputs, these being bond switching ($\kappa_2^{\Delta E}$), free volume (κ_2^{FV}) and bond metallicity (κ_2^{M}):

$$(1 - \kappa_2) = (1 - \kappa_2^{\Delta E}) \cdot (1 - \kappa_2^{FV}) \cdot (1 - \kappa_2^{M}). \qquad (2)$$

The bond switching input ($\kappa_2^{\Delta E}$) is defined by redistribution of covalent chemical bonds dependent on the balance between their dissociation energies [4,51]:

$$\kappa_2^{\Delta E} = \sum_i \frac{\eta_{1i} \cdot \eta_{2i}}{Y} \cdot e^{-\frac{\Delta E_i}{E_0}}\Big|_{\Delta E_i \geq 0}, \quad (3)$$

where ΔE_i is the energetic balance for the *i-th* bond-switching reaction selected via procedure [45]; E_0 is the initial linking energy of glass matrix; η_{1i} and η_{2i} are the respective fractions of bonds participating in this *i-th* bond-switching reaction, and Y is the normalization coefficient.

From energetic standpoint, the effect of short-wave shift in the optical absorption edge of ChSG is caused by bond-switching reactions with positive barrier $\Delta E > 0$, while bond-switching reactions with negative barrier $\Delta E < 0$ result in long-wave shift [4,52]. So, the residual effect of radiation-induced darkening should be associated with negative bond-switching reactions ($\Delta E < 0$).

The free-volume input (κ_2^{FV}) available for structural relaxation is most rigorous condition, which determines the metastability of RIEs in ChSGs [4,53-56]. In general, the close-packed atomic networks make possible faster relaxation of induced changes. Therefore, the density of glass ρ_g and isocompositional crystal ρ_{cr} can be used to estimate this input in an overall relaxation process:

$$\kappa_2^{FV} = 1 - \frac{\Delta\rho}{\rho_{cr}} = \frac{\rho_g}{\rho_{cr}}. \quad (4)$$

However, the ρ_{cr} cannot be found directly for ChSGs having no isocompositional crystals. In such a case, the ρ_{cr} values can be averaged from densities of nearest crystalline compositions. This is most controversial point, because the κ_2^{FV} values may be strongly governed by this choice. In g-As_xS_{100-x} system with known densities for all glass-forming compositions ($10<x<45$) [7,57,58], considered in connection with their crystalline counterparts such as sulphur S, As_2S_3 and some stable As-rich molecular crystals (As_4S_4 and As_4S_3), the highest κ_2^{FV} =0.098 is found for g-$As_{40}S_{60}$ (for comparison, the κ_2^{FV} extrapolated for As_4S_4 and As_4S_3 are 0.062 and 0.047, respectively).

Interestingly, to estimate free volume effect on RIEs in g-As(Ge)-S(Se) ChSGs, some authors use other parameter, defined as compactness multiplied by concentration of heteronuclear bonds, the former being calculated for ChSG decomposed on boundary elemental components [59-61]. Despite success of such approach in explaining photoinduced effects in some thin ChSG films, where homo-to-heteronuclear bonds disproportionality obviously takes place [62], this approach is rather limited because of more complicated structural motives in realistic glass-forming networks, which cannot be simplified by sum of boundary elemental components.

The bond metallicity input (κ_2^{M}) concerns DPTs stabilization in a glass network due to local electric charge distribution, like CTDs formation (when over-coordinated atom attains positive charge, and under-coordinated atom attains negative charge):

$$\kappa_2^{M} = \sum_i \alpha_{Mi} \cdot x_i. \quad (5)$$

where α_{Mi} and x_i denote the degree of electron delocalization (i.e. bond metallicity) and fraction of the *i-th* bond (after Harrison [63,64], each bond can be characterized by metallicity, covalency and iconicity, using specific bond energies dependent on atomic terms), respectively.

By applying this approach to g-As_xS_{100-x} characterized by chemically-ordered covalent-bonded networks [65-67] under condition of bond-switching reactions with negative barrier ($\Delta E < 0$) [4,52], we obtain for SM efficiency two distinct maxima near g-$As_{30}S_{70}$ and g-$As_{40}S_{60}$ as shown in Fig. 5. It seems this finding contradicts to optical transmission changes in g-As_xS_{100-x} measured *in-situ* in backward chronology (Fig. 4), showing single maximum for g-$As_{40}S_{60}$. But, this discrepancy can be simply explained by different weight of bond-switching reactions with negative barriers ($\Delta E < 0$).

In As-S system, there are three bond-switching reactions with $\Delta E < 0$ shown in Fig. 6, accompanied by (As_4^+,S_1^-) CTDs formation (where sub- and super-scripts are respectively used to denote local atomic coordination and electric charge excess) [4,52]. One can see from Fig. 5 that if

only hetero-to-homo-nuclear bond-switching reaction #6 (the numeration is accepted as in ref. [52]) with ΔE = -0.73 eV takes place, the κ parameter indeed shows obvious maximum near g-$As_{40}S_{60}$. This was indeed verified experimentally for g-$As_{40}S_{60}$ [4,14,15,68-70].

Thus, we conclude that bond-switching reactions #2 and #10 (see Fig. 6) are not responsible for residual RIEs in chemically-ordered covalent networks of g-As_xS_{100-x}.

4. Conclusions

In conclusive remarks, the methodological resolutions identifying unambiguously radiation-induced optical effects in chalcogenide semiconductor glasses should account for intrinsic and impurity-related destruction-polymerization transformations accompanied by post-irradiation physical ageing. The *ex-situ* optical measurements in *direct chronology* can be used to detect these changes, but they are ineffective to parameterize reliably radiation-optical response because of unavoidable drift in the sensitivity of detecting systems within prolonged and multiply repeated measuring cycles, unresolved input from natural and radiation-assisted physical ageing, and eventual mismatch between control and reference glass samples. It is convincingly shown that continuous *in-situ* optical measurements realized in *backward chronology* for preliminary irradiated glass provide an adequate signature of radiation-optical effect not biased by contribution from accompanied oxidation and thermally-induced ageing. These conclusions are well justified for g-$As_{40}S_{60}$ and g-$As_{30}S_{70}$ demonstrating principally different responses on intrinsic radiation-structural transformations and accompanied physical ageing. These methodological resolutions are in full agreement with structural modification criterion developed to parameterize compositional trends in metastable radiation-optical response of chalcogenide glasses.

Acknowledgement: OSh acknowledges support from Project No 0116U002578, subject of Scientific Program of the Ministry of Education and Science of Ukraine for 2016-2018. AK and RG admit financial support from NSF grant DMR-1409160. MSh acknowledges support from the Ministry of Education and Science of Ukraine within funding program DB/Nanosensor (No 0116U004411).

References

1. Starodubcev S.V., Domoryad I.A., Khiznichenko L.P. Changes of mechanical characteristics of amorphous selenium under gamma-ray influence. – Dokl. AN SSSR 139 (1961) 594-595.
2. Domoryad I.A., Kaipnazarov D., Khiznichenko L.P. Effect of gamma-irradiation on elastic properties of vitreous arsenic trisulphide. – Izv. AN Uzb.SSR. Ser. Fiz.-Mat. Nauk 5 (1963) 87-89.
3. Domoryad I.A., Kaipnazarov D. Effect of γ-irradiation on elastic properties of chalcogenide glasses of As_2Se_3-As_2Te_3 system. – Izv. AN Uzb.SSR. Ser. Fiz.-Mat. Nauk 3 (1964) 67-70.
4. Shpotyuk O.I. Chapter 6. Radiation-induced effects in chalcogenide vitreous semiconductors. In: Semiconducting Chalcogenide Glass I: Glass Formation, Structure, and Stimulated Transformations in Chalcogenide Glasses: Semiconductors and Semimetals, Vol. 78 (R. Fairman and B. Ushkov, eds.). Elsevier Academic Press, Amsterdam-Boston-London-New York-Oxford-Paris-San Diego-San Francisco-Singapore-Sydney-Tokyo, 2004, 215-260.
5. Gurevich S.B., Ilyashenko N.N., Kolomiets B.T., Lyubin V.M., Shilo V.P. Photostimulated changes of optical properties and structure of amorphous Se-As films. – Phys. Stat. Sol. A 26 (1974) K127-K130.
6. Kolomiets B.T., Lyubin V.M. Reversible photoinduced changes in the properties of chalcogenide vitreous semiconductors. – Mat. Res. Bull. 13 (1978) 1343-1350.
7. Feltz A. Amorphous Inorganic Materials and Glasses. – VCH Publ., Inc. Weinheim-New York-Basel-Cambridge-Tokyo, 1993, 1-446.
8. Shpotyuk O.I. Induced effects in chalcogenide glassy semiconductors and destruction-polymerization transformations concept. – Latv. J. Phys. Techn. Sci. 4 (1993) 32-43.
9. Shpotyuk O.I. Mechanism of radiation-structural transformations in amorphous As_2S_3. – Rad. Effects and Defects in Solids 132 (1994) 393-396.

10. Shpotyuk O.I., Matkovskii A.O. Radiation-stimulated processes in vitreous arsenic trisulphide. – J. Non-Cryst. Solids 176 (1994) 45-50.
11. Shpotyuk O.I., Kovalskiy A.P. Compositional trends in radiation-optical properties of chalcogenide glasses. – J. Optoelectron. Adv. Mater. 4 (2002) 751-762.
12. Shpotyuk O., Filipecki J., Shpotyuk M. Destruction-polymerization transformations as a source of radiation-induced extended defects in chalcogenide glassy semiconductors. – Phys. Stat. Sol. C 10 (2013) 125-128.
13. Shpotyuk Ya., Shpotyuk M. Radiation-induced effects in chalcogenide amorphous semiconductors: On the role of destruction–polymerization transformations. – J. Non-Cryst. Sol. 377 (2013) 46-48.
14. Shpotyuk M.V., Vakiv M.M., Shpotyuk O.I., Ubizskii S.B. On the origin of radiation-induced metastability in vitreous chalcogenide semiconductors: The role of intrinsic and impurity-related destruction-polymerization transformations. – Semicond. Phys. Quant. Electron. Optoelectron. 18 (2015) 90-96.
15. Frumar M., Firth A.P., Owen A.E. A model for photostructural changes in the amorphous As-S system. – J. Non-Cryst. Solids 59-60 (1983) 921-924.
16. Shpotyuk O.I. Spectroscopic investigations of penetrating radiation influence on the surface of vitreous arsenic chalcogenides in IR region. – Ukr. Phys. J. 32 (1987) 509-512.
17. Trubisky M.P., Neyhart J.H. Aging of vitreous arsenic-selenium photoconductors. – Appl. Opt. Suppl. 3 (1969) 59-63.
18. Shpotyuk M., Shpotyuk O., Serkiz R., Demchenko P., Kozyukhin S. Surface oxidation in glassy arsenic trisulphide induced by high-energy γ-irradiation. – Rad. Phys. Chem. 97 (2014) 341-345.
19. L.C.E. Struik, Physical ageing in amorphous polymers and other materials (Elsevier, New York, 1978).
20. Shieh S.H.M., LaCourse W.C. Ageing and sub-T_g relaxation in arsenic selenide glass fibers. – Materials Chem. Phys. 35 (1993) 160-167.
21. Nemilov S.V. Physical ageing of silicate glasses at room temperature: general regularities as a basis for the theory and the possibility of a priori calculation of the ageing rate. – Glass Phys. Chem. 26 (2000) 511-530.
22. Saiter J. M. Physical ageing in chalcogenide glasses. – J. Optoelectron. Adv. Mater. 3 (2001) 685-694.
23. Golovchak R., Gorecki Cz., Kozdras A., Shpotyuk O. Physical ageing effects in vitreous arsenic selenides. – Sol. State Commun. 137 (2006) 67-69.
24. Lucas P. Relaxation and fragility in chalcogenide network glasses. – Chapter 2 in: Amorphous Chalcogenides. Advances and Applications. Rongping Wang (Ed.). Taylor & Francis Group. 2013. P. 19-58.
25. Mouawad O., Strutynski C., Picot-Clémente J., Désévédavy F., Gadret G., Jules J.-C., Smektala F. Optical aging behaviour naturally induced on As_2S_3 microstructured optical fibres. – Opt. Mater. Express 4 (2014) 2190-2203.
26. Shpotyuk O., Golovchak R., Kozdras A. Chapter 8: Physical ageing of chalcogenide glasses. In: Chalcogenide glasses: Preparation, properties and applications (Eds. J.-L. Adam and X. Zhang). Woodhead Publ. Ser. in Electron. Optical Mater., Philadelphia-New Delhi, 2013, 209-264.
27. Golovchak R., Shpotyuk O., Kozdras A., Riley B.J., Sundaram S.K., McCloy J.S. Radiation effects in physical aging of binary As-S and As-Se glasses. – J. Therm. Anal. Calorim..103 (2011) 213-218.
28. Kavetskyy T.S. Radiation-induced optical darkening and oxidation effects in As_2S_3 glass. – Semicond. Phys. Quantum Electron. Optoelectron. 17 (2014) 308-312.
29. Kavetskyy T.S. Long-term radiation-induced optical darkening effects in chalcogenide glasses. – Semicond. Phys. Quantum Electron. Optoelectron. 19 (2016) 395-398.
30. Kavetskyy T.S., Stepanov A.L. Chapter 14: Effects of gamma-irradiation and ion implantation in chalcogenide glasses. – In: Glass Nanocomposites: Synthesis, Properties and Applications (Eds. B. Karmakar, K. Rademann, A.L. Stepanov). Elsevier Acad. Press, Amsterdam-Boston-Heidelberg-

London-New York-Oxford-Paris-San Diego-San Francisco-Singapore-Sydney-Tokyo, 2016, 341-358.
31. Shpotyuk M., Shpotyuk O., Golovchak R., McCloy J., Riley B. Compositional trends of γ-induced optical changes observed in chalcogenide glasses of binary As-S system. – J. Non-Cryst. Solids 386 (2014) 95-99.
32. Shpotyuk O., Ingram A., Szatanik R., Shpotyuk M., Golovchak R. Structural-relaxation phenomena in As-S glasses as probed by combined PAL/DBAR technique. – Mat. Chem. Phys. 155 (2015) 76-82.
33. Sundaram S.K., McCloy J.S., Riley B.J., Murphy M.K., Qiao H.A., Windisch C.F., Jr., Walter E.D., Crum J.V., Golovchak R., Shpotyuk O. Gamma radiation effects on physical, optical, and structural properties of binary As-S glasses. – J. Amer. Ceram. Soc. 95 (2012) 1048-1055.
34. Balitska V., Filipecki J., Shpotyuk O., Swiatek J., Vakiv M. Dynamic radiation-induced effects in chalcogenide vitreous compounds. – J. Non-Cryst. Solids 287 (2001) 216-221.
35. Shpotyuk O.I., Savitsky I.V. Radiation-thermal effects in vitreous semiconductors of As_2S_3-Sb_2S_3 system. – Ukr. Fiz. Zh. 34 (1989) 894-898.
36. Golovchak R.Ya., Shpotyuk O.I., Boyko V.T., Zurawska A. On the temperature behaviour of optical transmission spectra of γ-modified vitreous As_2S_3. – Ukr. J. Phys. Opt. 7 (2006) 18-23.
37. Berkes J.S., Ing S.W., Jr., Hillegas W.J. Photodecomposition of amorphous As_2Se_3 and As_2S_3. – J. Appl. Phys. 42 (1971) 4908-4916.
38. Keneman S.A., Bordogna J., Zemel J.N. Evaporated films of arsenic trisulfide: Physical model of effects of light exposure and heat cycling. – J. Appl. Phys. 49 (1978) 4663-4673.
39. Sanghera J.S., Busse L.E., Aggarwal I.D. Effect of scattering centers on the optical loss of As_2S_3 glass fibers in the infrared. – J. Appl. Phys. 75 (1994) 4885-4891.
40. Bohren C.F., Huffman D.R. Absorption and scattering of light by small particles. John Wiley & Sons, New York, 1983, 1-530.
41. Shpotyuk O.I., Golovchak R.Ya., Kovalskiy A.P., Vakiv M.M., Pamukchieva V.D., Arsova D.D., Skordeva E.R. Radiation-optical effects in As_2S_3-GeS_2 semiconducting glasses. – Phys. Chem. Glass. 42 (2001) 95-98.
42. Skordeva E., Arsova D., Pamukchieva V., Vateva E., Golovchak R., Kovalskiy A., Shpotyuk O. γ-induced changes in Ge-As-S glasses. – J. Optoelectron. Adv. Mater. 2 (2000) 259-266.
43. Lovas G., Mitsa V., Holomb R., Rosola I., Borkach E. The room temperature visible photoluminescence in g-As_2S_3 and Ge-based glasses. – Sci. Bull. Uzhgorod Univ. Ser. Fiz. 34 (2013) 54-58.
44. Tanaka K. Reversible photoinduced change in intermolecular distance in amorphous As_2S_3 network // Appl. Phys. Lett., 26, p. 243-245 (1975).
45. Golovchak R., Kozdras A., Shpotyuk O. Optical signature of structural relaxation in glassy $As_{10}S_{90}$. – J. Non-Crys. Solids 356 (2010) 1149-1152.
46. Tanaka K. Photoexpansion in As_2S_3 glass. – Phys. Rev. B 57 (1998) 5163-5167.
47. Popov A.I., Michalev N.I., Shemetova V.K. Structural modification of some glassy chalcogenides – Phil. Mag. B 47 (1983) 73-81.
48. Popov A.I., Domoryad I.A., Michalev N.I. Structural modification of arsenic chalcogenide glasses under γ-radiation. – Phys. Stat. Sol. A 106 (1988) 333-337.
49. Popov A. Structural characteristics and structural modifications of non-crystalline semiconductors. – J. Optoelectron. Adv. Mater. 4 (2002) 481-488.
50. Popov A. Chapter 2. Atomic structure and structural modification of glass in Semiconductors and Semimetals. In: Semiconducting Chalcogenide Glass I: Glass Formation, Structure, and Stimulated Transformations in Chalcogenide Glasses: Semiconductors and Semimetals, Vol. 78 (R. Fairman and B. Ushkov, eds.). Elsevier Academic Press, Amsterdam-Boston-London-New York-Oxford-Paris-San Diego-San Francisco-Singapore-Sydney-Tokyo, 2004, 51-96.
51. Shpotyuk M., Shpotyuk O., Kovalskyy A., Iovu M., Andriesh A. Post-technological structural modification route for network glass-forming systems. – Mold. J. Phys. Sci. 10 (2011) 82-88.
52. Golovchak R.Ya., Shpotyuk O.I. Radiation-induced bond switching in mixed Ge-As sulphide

glasses. – Phil. Mag. 85 (2005) 2847-2860.
53. Shimakawa K., Kolobov A., Elliott S.R. Photoinduced effects and metastability in amorphous semiconductors and insulators. – Adv. Phys. 44 (1995) 475-588.
54. Elliott S.R. A unified model for reversible photostructural effects in chalcogenide glasses. – J. Non-Cryst. Solids 81 (1986) 71-98.
55. Tanaka K., Shimakawa K. Amorphous Chalcogenide Semiconductors and Related Materials. Springer, New York-Dordrecht-Heidelberg-London, 2011, 1-242.
56. Photo-Induced Metastability in Amorphous Semiconductors. Ed. A. Kolobov. WILEY-VCH GmbH & Co. KGaA. Weinheim, 2003, 1-412.
57. Nemilov S.V. Viscosity and elastic properties of melts and glasses of As-S system and their valence structure – Glass Phys. Chem. 5 (1979) 398-409.
58. Borisova Z.U. Glassy Semiconductors. Plenum Press, New York-London, 1981, 1-505.
59. Vlcek M., Frumar M., Vidourek A. Photoinduced effects in Ge-Sb-S glasses and amorphous layers. – J. Non-Cryst. Solids 90 (1987) 513-516.
60. Vlcek M., Frumar M. Model of photoinduced changes of optical properties in amorphous layers and glasses of Ge-Sb-S, Ge-S, As-S and As-Se systems. – J. Non-Cryst. Solids 97-98 (1987) 1223-1226.
61. Frumar M., Cernosek Z., Jedelsky J., Frumarova B., Wagner T. Photoinduced changes of structure and properties of amorphous binary and ternary chalcogenides. – J. Optoelectron. Adv. Mater. 3 (2001) 177-188.
62. Mikhailov M.D., Karpova E.A., Cimpl Z., Kosek F. Photo- and thermally induced change in the volume of thin chalcogenide films. – Phys. Stat. Sol. A 117 (1990) 467-475.
63. Harrison W.A. Electronic structure and the properties of solids. The physics of the chemical bond. – Mir, Moscow, 1983, 1-571.
64. Harrison W.A. Theory of the two-center bond. – Phys. Rev. B 27 (1983) 3592-3604.
65. Yang C.Y., Paesler M.A., Sayers D.E. Chemical order in the glassy As_xS_{1-x} system: An X-ray-absorption spectroscopy study. – Phys. Rev. B 39 (1989) 10342-10352.
66. Golovchak R., Kovalskiy A., Miller A.C., Jain H., Shpotyuk O. Structure of Se-rich As-Se glasses by high-resolution x-ray photoelectron spectroscopy. – Phys. Rev. B 76 (2007) 125208-1-125208-7.
67. Bureau B., Troles J., LeFloch M., Smektala F., Silly G., Lucas J. Solid state 77Se NMR investigations on arsenic-selenium glasses and crystals. – Solid State Sci. 5 (2003) 219-224.
68. Yang C.Y., Paesler M.A., Sayers D.E. Measurement of local structural configurations associated with reversible photostructural changes in arsenic trisulfide films. – Phys. Rev. B 36 (1987) 9160-9167.
69. Kornelyuk V.N., Savitskii I.V., Shpotyuk O.I., Yaskovets I.I. Mechanism of reversible photoinduced effects in thin As_2S_3 films. – Phys. Solid State 31 (1989) 311-313.
70. Tichy L., Vidourek A., Nagels P., Callaerts R., Ticha H. On the origin of reversible photodarkening in amorphous As_2S_3 thin films. – Opt. Mater. 10 (1998) 117-129.

Figure captions:
Fig. 1. Methodological solutions for RIEs detection in ChGSs

Fig. 2. Optical transmission spectra of g-$As_{40}S_{60}$ (d≈1mm) detected *ex-situ* in direct chronology, showing two initial states for rejuvenated (solid-blue curve, state 1.1) and thermally-aged (solid-black curve, state 1.2) samples, two after-irradiation states for cleaned (solid-red curve, state 2.1) and uncleaned (thin-red curve, state 2.2) samples, and two thermally-aged states for irradiated cleaned (solid-black curve, state 3.1) and uncleaned (thin-black curve, state 3.2) samples.

Fig. 3. Optical transmission spectra of preliminary cleaned g-$As_{40}S_{60}$ (a) and g-$As_{30}S_{70}$ (b) samples (d≈1.5 mm) detected *in-situ* in *backward chronology* in γ-irradiated (1, black curve), then near-T_g annealed (2, red curve) and rejuvenated (3, blue curve) states.

Fig. 4. Compositional behavior of RIEs (~3 MGy) in g-As_xS_{100-x} exemplified by changes in optical transmittance due to longwave shift of fundamental absorption edge detected *in-situ* in backward chronology respectively to annealed ($T_{ann} - T_\gamma$) and rejuvenated ($T_{rej} - T_\gamma$) samples.

Fig. 5. The overall SM efficiency in g-As_xS_{100-x} obeying chemically-ordered covalent networks (bold circuits envelop curve) as originated from different bond-switching DPT reactions.

Fig. 6. Stick-and-ball presentation showing negative-barrier bond-switching reactions ($\Delta E < 0$) as selected from all possible DPTs in binary As-S system [4,52] responsible for reversible long-wave shift in optical absorption edge (see text for more details).

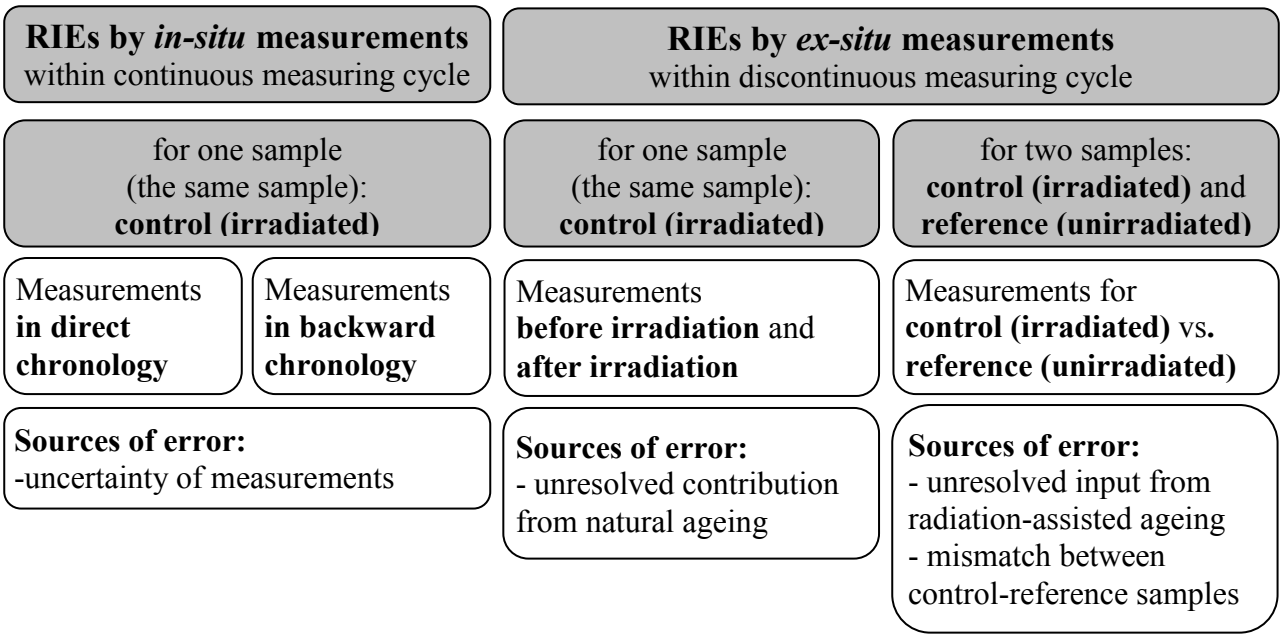

Fig. 1. Methodological solutions for RIEs detection in ChGSs.

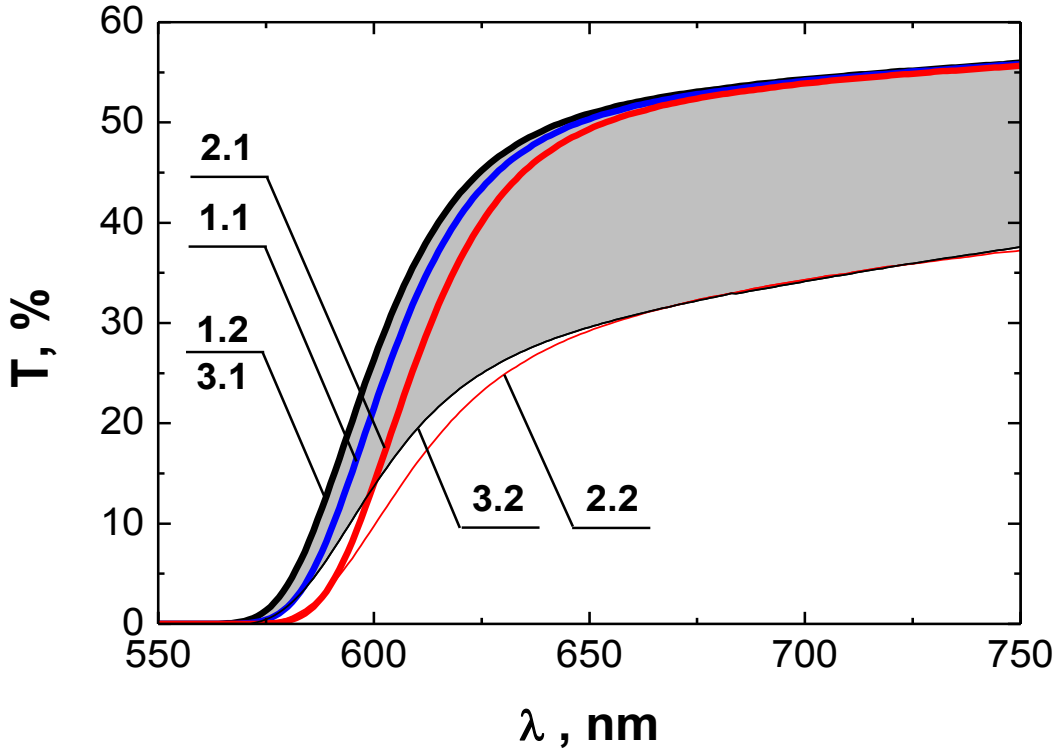

Fig. 2. Optical transmission spectra of g-$As_{40}S_{60}$ (d≈1mm) detected *ex-situ* in direct chronology, showing two initial states for rejuvenated (solid-blue curve, state 1.1) and thermally-aged (solid-black curve, state 1.2) samples, two after-irradiation states for cleaned (solid-red curve, state 2.1) and uncleaned (thin-red curve, state 2.2) samples, and two thermally-aged states for irradiated cleaned (solid-black curve, state 3.1) and uncleaned (thin-black curve, state 3.2) samples.

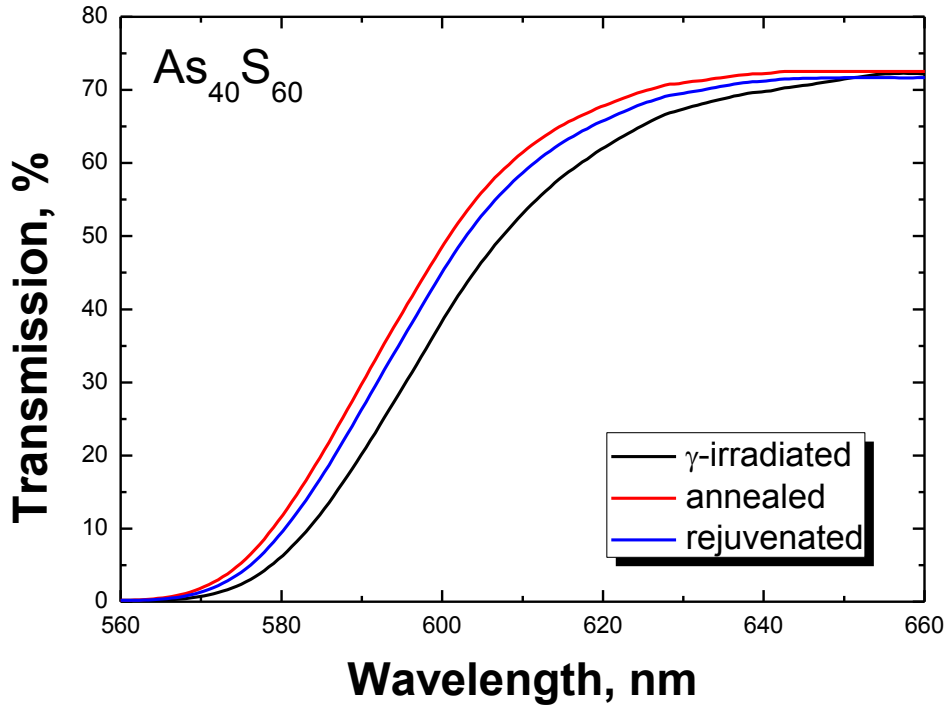

a

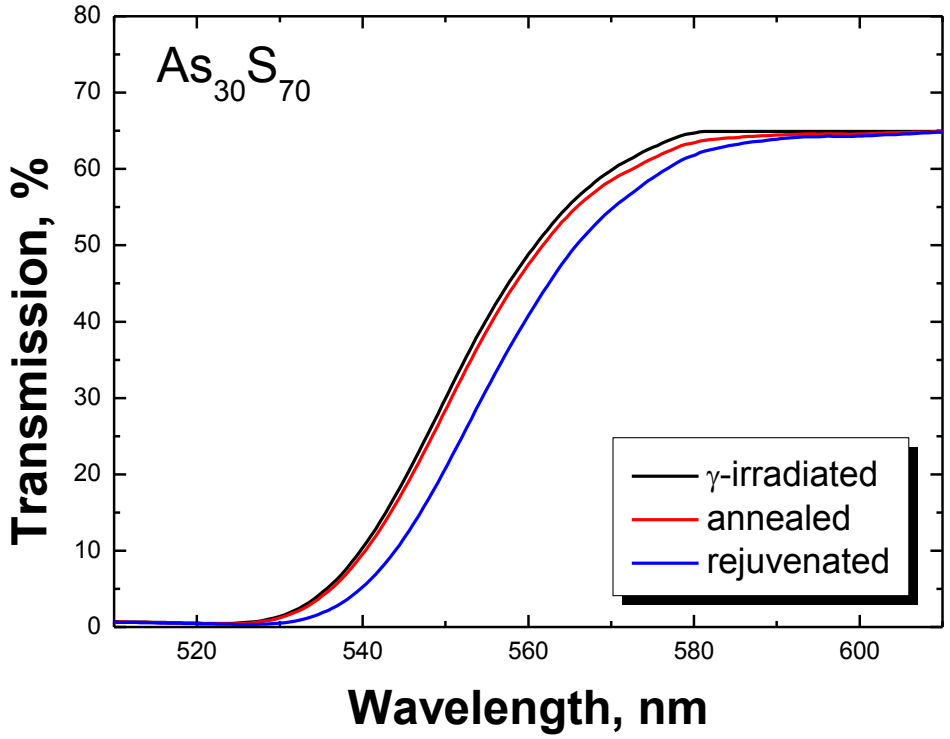

b

Fig. 3. Optical transmission spectra of preliminary cleaned g-$As_{40}S_{60}$ (a) and g-$As_{30}S_{70}$ (b) samples (d≈1.5 mm) detected *in-situ* in *backward chronology* in γ-irradiated (1, black curve), then near-T_g annealed (2, red curve) and rejuvenated (3, blue curve) states.

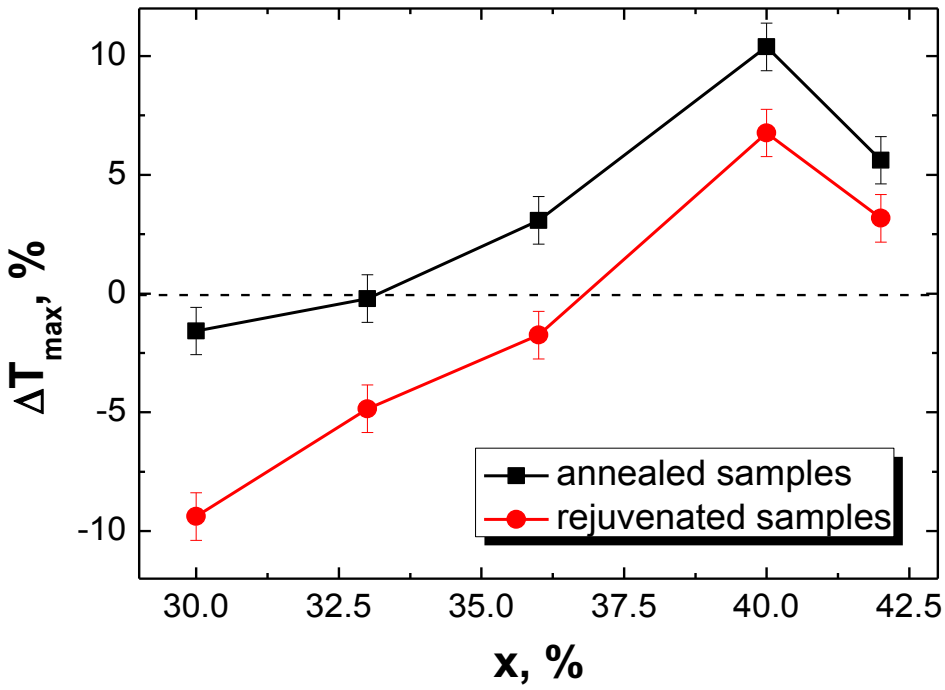

Fig. 4. Compositional behavior of RIEs (~3 MGy) in g-As_xS_{100-x} exemplified by changes in optical transmittance due to longwave shift of fundamental absorption edge detected *in-situ* in backward chronology respectively to annealed ($T_{ann} - T_\gamma$) and rejuvenated ($T_{rej} - T_\gamma$) samples.

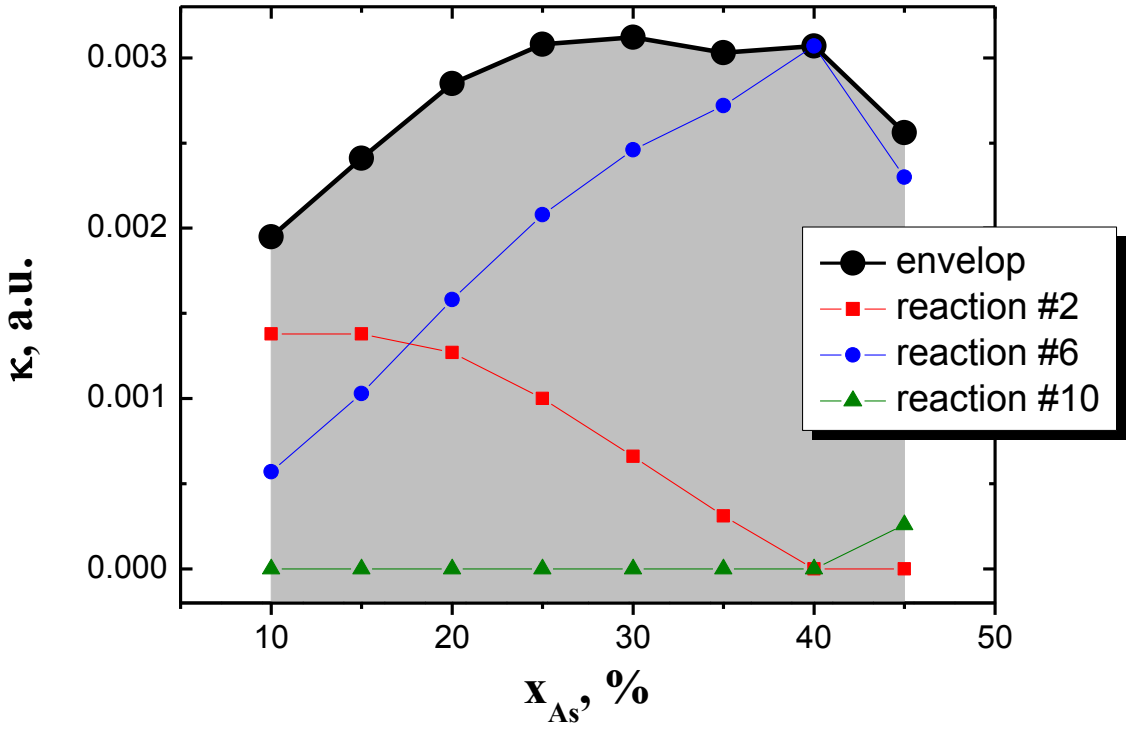

Fig. 5. The overall SM efficiency in g-As_xS_{100-x} obeying chemically-ordered covalent networks (bold circuits envelop curve) as originated from different bond-switching DPT reactions.

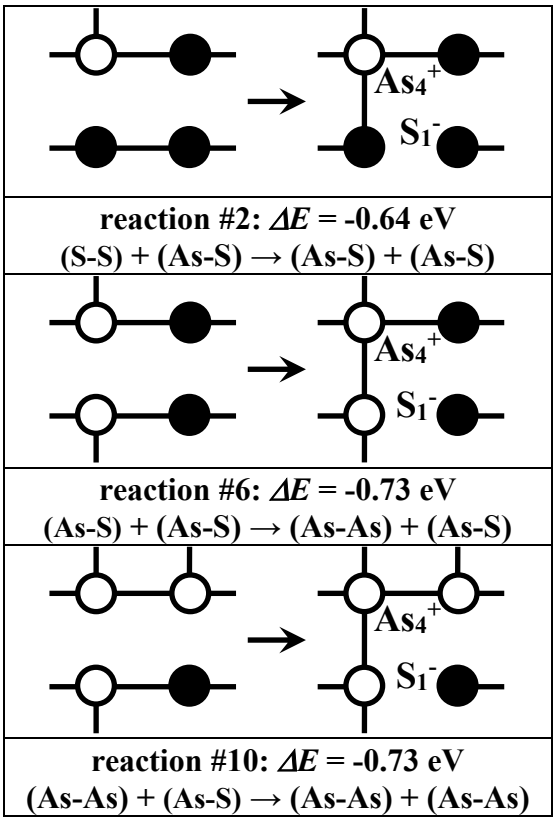

Fig. 6. Stick-and-ball presentation showing negative-barrier bond-switching reactions ($\Delta E < 0$) as selected from all possible DPTs in binary As-S system [4,52] responsible for reversible long-wave shift in optical absorption edge (see text for more details).